Temperature-Dependent Ultraviolet Resonance Raman Spectroscopy of the Premelting State of dA · dT DNA

Shirley S. Chan,* Robert H. Austin,* Ishita Mukerji,# and Thomas G. Spiro§

*Physics Department, Princeton University, Princeton, New Jersey 08544; #Department of Molecular Biology and Biochemistry, Wesleyan University, Middletown, Connecticut 06459; and §Chemistry Department, Princeton University, Princeton, New Jersey 08544 USA

ABSTRACT Poly(dA) · poly(dT) and DNA duplex with four or more adenine bases in a row exhibits a broad, solid-state structural premelting transition at about 35°C. The low-temperature structure is correlated with the phenomena of "bent DNA." We have conducted temperature-dependent ultraviolet resonance Raman measurements of the structural transition using poly(dA) · poly(dT) at physiological salt conditions, and are able to identify, between the high and low temperature limits, changes in the vibrational frequencies associated with the C4 carbonyl stretching mode in the thymine ring and the N6 scissors mode of the amine in the adenine ring of poly(dA) · poly(dT). This work supports the model that the oligo-dA tracts' solid-state structural premelting transition is due to a set of cross-strand bifurcated hydrogen bonds between consecutive dA · dT pairs.

INTRODUCTION

It has been found that poly(dA) · poly(dT) and kinetoplast DNA fragments (kDNA) with phased oligo-dA tracts have a unique temperature-dependent structure well below the global melting point of the duplex and in the vicinity of physiological temperatures.

The broad temperature range over which the structure changes can be monitored by observing differential absorption spectra centering around 290 nm (Herrera and Chaires, 1989), circular dichroism (CD) spectra (Herrera and Chaires, 1989; Chan et al., 1990), gel mobility change (Chan et al., 1990), transient optical techniques (Chan et al., 1990), and the allosteric cooperative binding effect of drug to poly(dA) · poly(dT) (Herrera and Chaires, 1989). The low temperature structure of poly(dA) · poly(dT) is probably responsible for the anomalous gel mobility observed in DNA fragments containing phased A-tracts (Diekmann and Wang, 1985; Hagerman, 1986; Stellwagen and Stellwagen, 1990; Crothers and Drak, 1992).

Chan et al. (1990) showed by using CD spectra that this structural transition is characterized by four clean isoelliptic points throughout the transition; thus it is quite certain that the transition is between two clearly defined helical structural states rather than a gradual relaxation of the structure. The transition is independent of DNA duplex concentration and thus is intramolecular. The midpoint of this transition is centered around 35 ± 5°C. A 45-bp DNA duplex with four phased tracts of $(dA)_5$ spaced by randomized 5(GC) bases was designed to simulate a short segment of kDNA fragments. The heat capacity change ΔC_p associated with this preglobal melting transition has been measured by differential scanning calorimetry (DSC), so that direct thermodynamic information is available (Chan et al., 1993). The premelting transition was found to release enthalpy equivalent to a hydrogen type of bonding (about 4.4 ± 0.6 kcal/mol of AA step) for this phased 45-bp duplex.

X-ray crystallographic evidence has always pointed to the unusual amount of propeller twisting between the dA · dT base planes (20–30°) that is unique to the tracts of homo-dA · dT regions (Nelson et al., 1987; Coll et al., 1987; Yoon et al., 1988; Aymami et al., 1989). It has given hints of a candidate within the DNA duplex A-tract for this anomalous property: three-centered hydrogen bonds, also known as bifurcated H bonds, which can form only in A-tracts if the bases are allowed to propeller twist. Fig. 1 *a* shows the assignments of A-T base pair atoms, the two Watson-Crick H bonds, and the positions of the grooves. The 3-centered hydrogen is the hydrogen from the amine group (N6) of adenine, which links the oxygen of the carbonyl group (C4═O) of the Watson-Crick pairing thymine and the carbonyl oxygen (C4═O) of the thymine at the nearest neighbor. This geometry is possible *only* over a sequence element with three or more A-T pairs. Fig. 1 *b* shows a schematic diagram of these bonds. Notice that these carbonyl and amine groups are on the major groove side of the double helix. Fig. 1 *c* shows a color ball-stick view of the Nelson's deodecamer duplex structure (5′-CGCAAAAAAGCG and 5′-CGCTTTTTTGCG) (1987). We have added one H bond (*dashed line*) to represent the location of this third bond between the two strands in the $(dA)_6$-$(dT)_6$ region. In Fig. 1 *d*, using part of the deodecamer's coordinates, we have further zoomed in on the H bonds and the proximity between three pairs of A-T bases by adding the hydrogen atoms to N6. It is clear that it is physically possible to form this cross-strand bond.

The simple two-state model then would imply that at low temperature the base pairs are propeller-twisted and form the third H bond, balancing the mechanical strain energy of base-pair twist with the electronic energy gain in hydrogen bond formation. At high temperatures this H bond breaks

Received for publication 22 April 1996 and in final form 8 January 1997.

Address reprint requests to Prof. Robert H. Austin, Physics Dept., Princeton University, P.O. Box 708, Princeton, NJ 08544-0708. Tel.: 609-258-4353; Fax: 609-258-1115; E-mail: rha@suiling.princeton.edu.

0006-3495/97/04/1512/09 $2.00

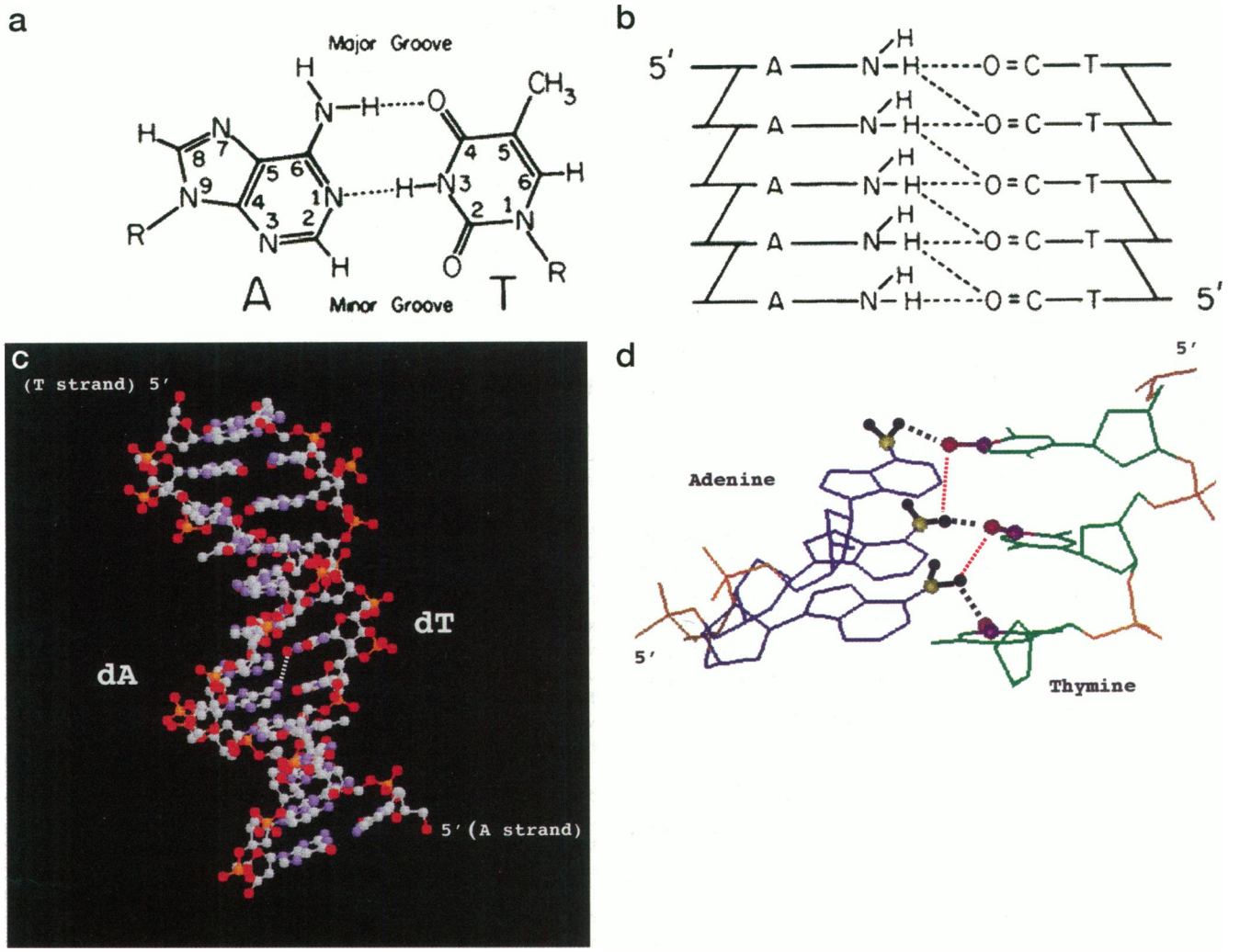

FIGURE 1 (*a*) The Watson-Crick base pairing of adenine and thymine. (*b*) The schematic of the bifurcated H bond between A_n-track and T_n-track. (*c*) The three-dimensional X-ray structure of the Nelson deodecamer (Nelson et al., 1987). Atoms in red are oxygen, blue are nitrogen, and grey are carbon. Only one bifurcated bond between C4═O and N6—H is shown as a dashed line, to demonstrate its location and proximity. (*d*) A rotated and enlarged view of *c*, with only three A-T pairs and with added hydrogen atoms, showing the position of the bifurcated bond as a small dashed line.

and the strain in the helix is released to a more coplanar configuration, which would be the canonical B type. A true molecular understanding of this structural transition is necessary if we are to understand the basic rules by which noncoding DNA sequences control DNA expression. Thus the questions we ask and try to answer in this communication are: What are the base-pair-specific origins of the structural metastability and the source of the enthalpy change?

UV RESONANCE RAMAN

Testing of this model requires a physical probe sensitive to the formation of the 3-centered bond. Although conventional Raman spectroscopy is somewhat sensitive to changes in bond order, the complex chemical composition of duplex DNA and scattering from the solvent makes it difficult to find changes within a forest of vibrational bands. However, resonance Raman spectroscopy allows one to preferentially examine the vibrational modes from a group if it has an electronically allowed transition distinct from other groups. By using an ultraviolet (UV) excitation wavelength where the DNA bases absorb, all of the Raman bands associated with the base rings will be enhanced over those associated with the phosphate and sugar backbones, as well as those from the buffer and solvent (Fodor et al., 1985; Fodor and Spiro, 1986; Tsuboi et al., 1987; Perno et al., 1989; Toyama et al., 1991). Thus UV resonance Raman (UVRR) provides a mean for identifying subtle changes in bond order and conformation by monitoring spectral changes. We stress, however, that although UVRR spectroscopy can be used to find changes in the bond order, the relatively low signal/noise of the technique, the extensive averaging and large sample size, and the subtle changes in the lines observed preclude using UVRR to map out in detail the temperature dependence of the structural transi-

tion. We feel that the evidence for a structural transition has been amply documented in our work and other experiments cited above. Rather, it is the purpose of this communication to show that at the extreme points of the transition, clearly identifiable and understandable changes in the UVRR spectrum are observable.

We begin our discussion with a brief review of the assignment of the UVRR transitions. The exocyclic carbonyl and amino groups make the dominant contributions to the bands in the high-frequency range (1550–1750 cm^{-1}) of the Raman spectra. Moreover, it has been shown by Spiro and his colleagues (Fodor et al., 1985; Fodor and Spiro, 1986; Perno et al., 1989) that in dTMP and in A-T polymers, if the UVRR is done near 260 nm, the thymine C4═O vibration is seen as a strong, broad band at around 1650 to 1690 cm^{-1}, but the C2═O vibration is not. This is due to the electronic dipole moment centered on the C6═C5—C4═O enone fragment of the thymine ring being strongly vibrationally coupled to 260 nm, whereas the C2═O vibration is weakly coupled by vibrations orthogonal to the electronic dipole axis. Moreover, the C6═C5 stretch lies close to the C4═O stretch to form a broad asymmetrical band that could be difficult to resolve (Fodor et al., 1985; Grygon and Spiro, 1990). However, it is important to note that by using UVRR enhancement at appropriate excitation wavelengths, transitions of interest are selectively picked out and the band assignments could be simplified because nonenhanced transitions such as the adenine C6═N stretch, which could be confused with the thymine C4═O stretch, are simply not present (Toyama et al., 1991).

Whereas the ring modes are much less sensitive or insensitive to environments, the carbonyl stretch is sensitive to the change of H-bond strength and possibly any diople coupling of a neighboring carbonyl group (Tsuboi and Takahashi, 1973). For example, Toyama et al. (1991) have shown that in UVRR spectra of 1-methylthymine (MeT), a broad band at 1665 cm^{-1} is resolved into two bands when less polar solvents are used. The C4═O frequency shifts from 1665 cm^{-1} in water to 1668 cm^{-1} in methanol and to 1689 cm^{-1} in dioxane, whereas the C═C stretching frequency remains at 1661 cm^{-1}. From the IR spectrum, C4═O of MeT is observed at 1690 cm^{-1} in dioxane. In short, the thymine C4═O stretch is observed anywhere from 1650 to 1690 cm^{-1}, depending on the extent of H bonding from the environment.

The C2═O is located in the minor groove, and its stretching mode, which is best observed with shorter excitation wavelengths (200 to 218 nm) (Fodor et al., 1985), is near 1700 cm^{-1} as a weak band in dTMP, but is in the noise for polymers (Grygon and Spiro, 1990). From the IR spectrum of MeT in dioxane, the C2═O stretch is observed at 1711 cm^{-1} (Toyama et al., 1991). So the C2═O stretch, if observed, is well separated from the C4═O stretch.

Furthermore, the amino group at C6 of adenine is situated in the major groove, and its scissors mode is uniquely located at 1605 cm^{-1} for dAMP and polymers in aqueous conditions (Tsuboi et al., 1987; Grygon and Spiro, 1990; Toyama et al., 1991). The band has been found to be sensitive to changes in H-bonding and solvent conditions, especially those resulting from deuterium exchange.

Thus UVRR can provide a reasonably clean test for 3-centered hydrogen bond formation: observation of changes in the stretching frequency associated with thymine C4═O vibration around 1650–1690 cm^{-1}, plus any concomitant changes with the scissors mode of the amine group from adenine at 1605 cm^{-1} as the temperature is increased through the premelting transition region.

EXPERIMENTAL PROCEDURES

The polymer duplexes, poly(dA) · poly(dT) and poly[d(AT)], were purchased from Pharmacia and dissolved in the same standard buffer as in CD and DSC experiments (Chan et al., 1990, 1993). The buffer, always passed through a 0.2-μm filter before use, contained 10 mM sodium phosphate (pH 7.5), with 100 mM NaCl, a physiological salt range, and 10 μM disodium EDTA, which is denoted as DSC buffer. The alternating copolymer sample contained an additional amount of disodium sulfate (0.3 M) because the sulfate symmetrical stretch mode could be used as an internal standard for Raman spectral intensity and frequency. However, sulfate salt was not added to homopolymer sample to avoid any possibility of forming a triple helical complex at an elevated sodium concentration during the following annealing step. All samples were heated to about 95°C in a large water bath and slowly annealed over several hours at about 60–70°C before cooling down to room temperature over half a day.

Each sample was first checked by UV (260 nm) melting behavior from 5 to 95°C to verify that the sample had only one transition from helix to coil occurring above 65°C. Furthermore, aliquots of samples were always taken for gel analysis and comparison before and after Raman measurements. The concentration of the duplexes was adjusted to an optical density (OD) of about 20 at 260 nm, i.e., about 1 mg/ml. The volume used in the experiment was 1.5 ml. The sample in a magnetically stirred quartz cuvette was maintained at specified temperature with an aluminum block cuvette holder and circulating bath, with the sample temperature monitored by a copper constantin thermocouple in the block.

Laser radiation of 7-ns-wide pulses was generated by frequency doubling the output of a 300-Hz excimer-pumped dye laser (Lambda Physik LPX130/FL3002). To generate 260-nm light, Coumarin 521 (Exciton) was used as the lasing dye. UV radiation at an average power of 0.3 mW was incident on the sample, with a 135° backscattering geometry. The low power of the laser and the constant stirring of the sample ensured that sample local heating or radiation damage was not a problem.

A Spex 1.25-m single-monochromator spectrograph was used, coupled to an intensified diode array detector of 1024 channels. The spectral resolution of the instrument was 0.7 cm^{-1}/channel, covering about 700 cm^{-1} of spectrum. Each spectrum was accumulated over half an hour to achieve good signal-to-noise. Because intense UV light is used as the excitation source in these experiments, run times where limited to a time scale over which there was no noticeable degradation of the sample, as would be evidenced by discoloration. However, it was not thought advisable to do a long series of temperature-dependent runs or to attempt to reuse the sample many times.

The Raman band at 1421 cm^{-1} is assigned to the dexoyribosyl backbone (Peticolas and Evertsz, 1992), and it experiences little resonance enhancement. To generate the difference spectra, the intensity of this 1421 cm^{-1} peak was normalized to unity in each spectrum, and it was assumed that its intensity was unchanged at all of the temperatures examined.

Fitting was done using the software package Kaleidograph over the wavenumber range 1550–1750 cm^{-1}, by assuming that the data consisted of five Lorentzian peaks with variables: center frequency (ν), width (FWHM), and amplitude. The area under the peak was calculated as the percentage of the five fitted peaks. Lorentzians were found to give a

substantially better χ^2 than Gaussians, indicating that the peaks are transform-limited resonance scattering curves and not heterogeneously broadened. The data can also be fit with four Lorentzians and similar χ^2 values, but these fits result in a broad band at highest frequency with a linewidth over 50 cm^{-1}. Because a 50 cm^{-1} linewidth corresponds to a very short vibrational lifetime of approximately 100 fs, which is rather unphysical, we retained the five Lorentzian fits as the minimum number of physically reasonable peaks that could fit the data. The χ^2 values for the five-peak fits are reduced by at least 50% compared to the four-peak fits and the widths at half maxima (FWHM) of all peaks in the more realistic range of 12–36 cm^{-1}.

Evaluation of a true χ^2 is difficult, because the noise in the data is not due to counting statistics but rather diffuse scattering, readout, and electronic noise, which can change from run to run. As a best guess of the true data variance, which is heavily biased toward high-frequency noise, we subtracted a file from itself after shifting the wavelength origin by 3 cm^{-1}. The resulting curve consists mostly of high-frequency noise. The data variance σ, assumed to be independent of wavenumber, was then calculated by finding a region where there was little change in the scattering signal with photon energy and evaluating the sample variance σ. This variance was then used to calculate the reduced χ^2 of the fit versus the data:

$$\chi^2 = \sum_{i=1}^{N} \frac{[f(\nu) - s(\nu)]^2}{\sigma^2(N - 1 - n)}, \quad (1)$$

where N is the number of data points, $f(\nu)$ is the fitting function, $s(\nu)$ is the signal as a function of the wavenumber ν, and n is the number of independent degrees of freedom used in the fitting function. Error bars for the fit values are usually overoptimistically determined by most statistical packages because they assume truly random errors, which is rarely the case. In our case, the statistical estimate of the errors was approximately ± 0.1 cm^{-1} for the peak positions. However, rather than quote the error bars determined by the fitting algorithm, we feel from our experience with multiple runs that the peaks are known to ± 0.5 cm^{-1} in terms of run-to-run reproducibility.

RESULTS OF UVRR

The melting curves were first obtained to determine the midpoint of helix-coil transition at about 70°C for poly(dA) · poly(dT) in DSC buffer and for poly[d(AT)] in DSC buffer with added sulfate (data not shown). Because the midpoint of the premelting transition is about 35°C, we measured the UV resonance Raman spectra at 5°C (which represents the lowest temperature point), at 35°C, and at 55°C (which represents the highest temperature point before the onset of the duplex melting process). We examined both the homopolymer and alternating copolymer dA · dT duplexes and the spectral changes at these three temperatures. These Raman spectral changes are inherently small compared to the previously reported thermodynamic and optical activity changes (Herrera and Chaires, 1989; Chan et al., 1990) or gel mobility changes (Chan et al., 1990). Thus, for clarity of viewing, we only plot the spectra taken at the high and low temperature points. Although we did carry out an intermediate temperature run at 35°C, the data are not sufficiently different from the two extreme temperature runs to merit detailed analysis. It is unfortunate that the UVRR signal is not more drastically differentiated between the two temperatures; the subtle structural variations that can often give rise to large biological consequences are not easily detected by physical techniques sensitive mainly to large changes in bond order.

The coplot of 5°C and 55°C spectra of poly[d(AT)] is shown in Fig. 2 *a*. We have utilized the peak at 1421 cm^{-1}, which has been assigned to the ribosyl vibrational mode as our normalization factor, because this peak experiences little resonance enhancement. It exhibits little to no hypochromicity between these two temperatures. The difference spectrum between 5°C and 55°C is shown in Fig. 2 *a* below the coplot. At the high-frequency end, the three peaks above 1550 cm^{-1} show a slight uniform intensity decrease from low to high temperature and more importantly show no frequency shift at all. At the low-frequency end, the band at 1252 cm^{-1}, which is associated with the N1=C6 bond and

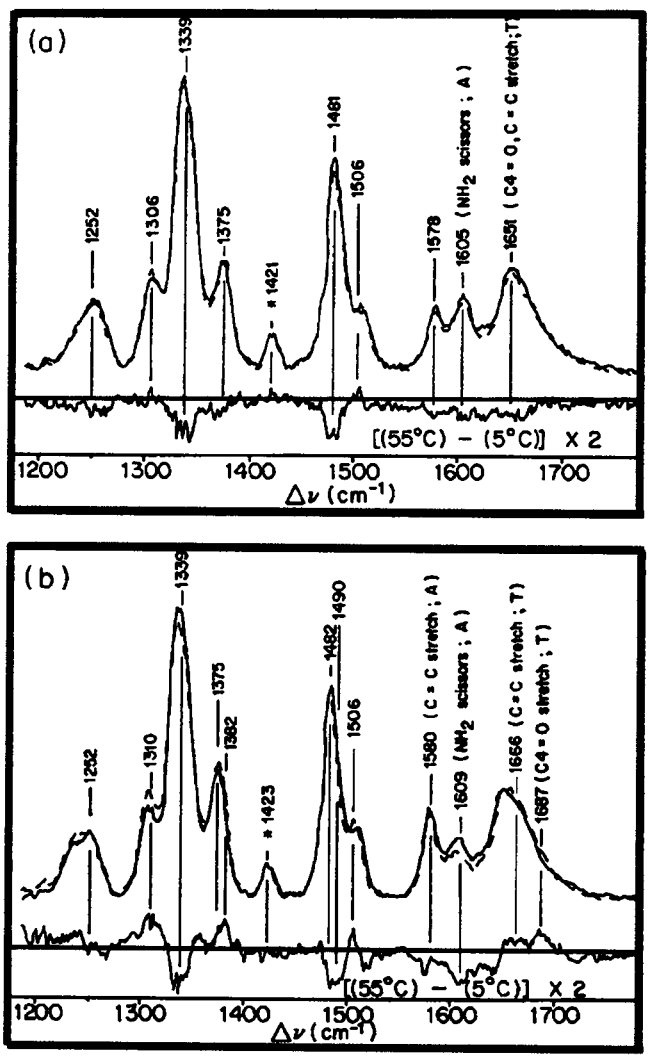

FIGURE 2 (*a*) The top curves are the overlay of UVRR spectra of poly[d(AT)] at 5°C (*solid line*) and at 55°C (*dashed line*). The bottom curve is the difference spectrum between 55°C and 5°C, amplified by a factor of 2. (*b*) The top curves are the overlay of UVRR spectra of poly(dA) · poly(dT) at 5°C (*solid line*) and at 55°C (*dashed line*). The bottom curve is the difference spectrum between 55°C and 5°C, amplified by a factor of 2. In both sets of spectra, the 1423 cm^{-1} peaks were used as the normalization for subtraction.

the C6—N6 bond of the adenine ring at 5°C, is the same as at 55°C. In previous work with 9-ethyladenine, this mode has been shown to be sensitive to hydrogen bonding at the exocyclic NH_2 acceptor sites (Toyama et al., 1991). This is further evidence of no change in hydrogen bonding at this location.

There are two sets of bands in the midrange that are not completely subtracted to zero: one is around 1339 cm^{-1} and the other is around 1481 cm^{-1}. The 1339 cm^{-1} band has been assigned to the stretching of C8═N7 and N7—C5 of adenine (Fodor et al., 1985). It is known to show a frequency shift of up to 7 cm^{-1} if all of the hydrogen bonds disrupt at N1, N3, and N7 (Toyama et al., 1991). Our difference spectrum shows only a decrease in intensity, and no shift in frequency for poly[d(AT)]. This kind of change implies that the vibrational band has been thermally broadened or experienced weak changes in hyperchromaticity due to changes in stacking interactions, but the nature of the hydrogen bond between N1 of adenine to N3 of thymine has not changed. In the second set of bands around 1470–1520 cm^{-1}, these have been assigned to the vibrations in the five-membered ring of the adenine (Thomas and Livramento, 1975) and to the out-of-phase stretches of thymine ring bonds coupled to C2—N1 and C2—N3 (Fodor et al., 1985). More specifically, the peak at 1481 cm^{-1} has been assigned to the adenine ring stretching of N9—C8 and bending modes of C2—H and C8—H (Fodor et al., 1985). The changes here are mostly in intensity, not frequency shift, and therefore can be attributed, similarly, to thermal broadening of each group of vibrational mode.

Overall, the essentially flat difference spectrum of alternating copolymer between 5°C and 55°C serves as a control for both the experimental set-up and the behavior of poly[d(AT)] base pairs, i.e., there is no temperature-dependent change below the duplex melting state.

The data are different for the homopolymer dA · dT. The coplot at 5°C and 55°C of poly(dA) · poly(dT) in DSC buffer is shown in Fig. 2 *b*. Again, the ribosyl band at 1423 cm^{-1} has been used as the normalization band. The spectrum shows definite shifts of the bands at the high-frequency region (1550–1750 cm^{-1}) and at lower frequency regions (~1382 cm^{-1} and ~1252 cm^{-1}). The difference spectrum between the two temperatures is shown below the coplot in Fig. 2 *b* and is definitely different from the alternating copolymer.

We first discuss the region below 1550 cm^{-1} for poly(dA) · poly(dT). The band at 1482 cm^{-1} shows an intensity decrease similar to that of the poly[d(AT)], whereas the side bands show further changes, primarily in intensity and not in frequency. These changes can be explained by thermal broadening, and there are no changes in H bonding around the adenine five-membered ring. The decrease in intensity at 1339 cm^{-1} also indicates thermal broadening, not any changes from H bonding associated with N1, N3, and N7. These two bands thus serve as a good control of the nonchanging status for the bonds within the adenine rings, especially the Watson-Crick H bond between N1 and thymine N3—H.

On the other hand, the broad band at 1252 cm^{-1}, which is a mixture of the adenine exocyclic C6—N6 bond and the N1═C6 ring bond, shows changes between high and low temperatures. The 1375 cm^{-1} band involves the out-of-phase stretches of thymine ring bonds coupled to C4═O, which is strongly enhanced by 260 nm excitation (Fodor et al., 1985). Thus the observed change at 1382 cm^{-1} could be coupled with thymine C4═O change.

Clearly the most significant changes between 5°C and 55°C in poly(dA) · poly(dT) occur above 1550 cm^{-1}, where the band assignments are less complicated and the frequencies directly measure the strength of adenine $N6H_2$ scissors mode and thymine C4═O stretch mode. There are two narrow bands (about 1580 cm^{-1} and 1609 cm^{-1}) and one broad band (about 1660 cm^{-1}), which are less convoluted than the multiple bands around 1252 cm^{-1} and around 1300–1390 cm^{-1}. We will concentrate in the data analysis and discussions on this high-frequency region for both polymer duplexes.

DETAILED ANALYSIS

We have plotted the high-frequency region (1550–1750 cm^{-1}) on an expanded scale. Fig. 3 *a* is for poly[d(AT)] at 5°C and Fig. 3 *b* is at 55°C. Fig. 4 *a* is for poly(dA) · poly(dT) at 5°C and Fig. 4 *b* is at 55°C. To curve fit this set of peaks with an emphasis on detecting frequency shifts, we have first normalized, with an intensity of peak around 1650 cm^{-1} to unity, and performed a Lorentzian fit to each spectrum. To obtain some realistic bandwidths for each resolved peak, it is necessary to use five peaks to fit this entire range. The parameters for the five peaks are found and summarized in Table 1 for poly[d(AT)] and Table 2 for poly(dA) · poly(dT).

Two of these peaks, 1578 and 1605 cm^{-1}, arise from adenine residues, whereas the remaining three are from thymine. The 1578 cm^{-1} mode is a ring vibration, with a large C4═C5 contribution, and the 1605 cm^{-1} mode is primarily the $-NH_2$ scissors vibration (Fodor et al., 1985). The three thymine peaks are part of a broad asymmetrical band at about 1660 cm^{-1}, which is known to contain components from separate C4═O and C5═C6 stretching modes (Fodor et al., 1985; Grygon and Spiro, 1990). However, the C4═O stretch is subject to dipole coupling between oscillators on different residues (Tsuboi, 1985; Tsuboi and Nishimura, 1982), and we assign the 1650 and 1685 cm^{-1} peaks to in-phase and out-of-phase stretches, $(C4{=}O)_A$ and $(C4{=}O)_B$; the 1667 cm^{-1} peak is assigned to the C5═C6 stretch. Evidence of a dipole-dipole effect on C═O stretching frequencies in polynucleotides includes noncoincidence of Raman and infrared bands (Tsuboi, 1985) and complex frequency shifts upon base-pair formation (Fodor and Spiro, 1986; Grygon and Spiro, 1990). The in-phase and out-of-phase modes are expected to have dis-

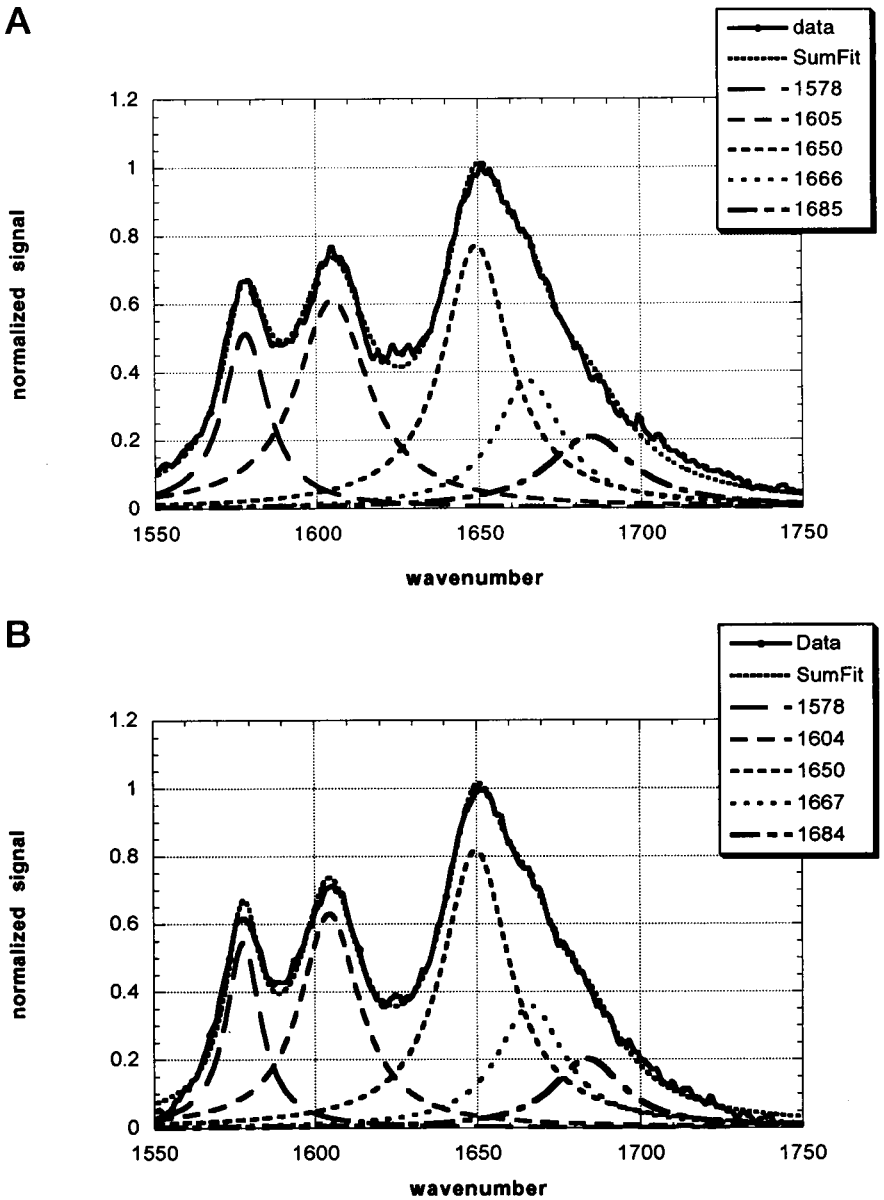

FIGURE 3 UVRR spectra from 1550 to 1750 cm^{-1} of poly[d(AT)] with Lorentzian fits using five peaks (*a*) at 5°C and (*b*) at 55°C. Solid lines are the data. All dash and dotted-dashed lines are the curve fits, and the dotted lines are fits to the data, made by summing the five peaks. The reduced χ^2 is 3.0 for *a* and 2.6 for *b*.

parate Raman and infrared intensities, and are not easy to detect in a single spectrum. This is the first UVRR study in which sufficient data have been collected to permit deconvolution of the out-of-phase C4═O component in the tail of the broad thymine band.

Interestingly, the distance between closest C4═O groups is almost the same, 3.8–4.0 Å in poly[d(AT)] and in poly(dA) · poly(dT), as revealed by the fiber diffraction data (Arnott and Selsing, 1974; Arnott et al., 1974). This coincidence accounts for the initially surprising result that the C4═O frequencies are the same at 55°C for the two polymers (Tables 1 and 2).

As expected, the five peaks for poly[d(AT)] have almost identical frequencies at 5°C (1578.1, 1605.1, 1649.5, 1665.5, and 1684.5 cm^{-1}) and at 55°C (1577.9, 1604.6, 1649.8, 1666.6, and 1684.0 cm^{-1}). The differences in frequency between two temperatures are $\delta\nu = 1$ cm^{-1} or less, well within experimental or fitting error. The fits confirm the notion that there are no bond changes attributable to the vibrational groups in this region, and hence no significant changes in the helical structure or bonding between the two temperatures.

However, the fitting results are very different for homopolymer poly(dA) · poly(dT). The first peak associated with the C4═C5 stretch of adenine shows, to within experimental error, essentially no frequency change with temperature (1579.5 cm^{-1} at 5°C and 1579.9 cm^{-1} at 55°C). The second peak from the scissors mode of adenine $N6H_2$ shows a clear frequency downshift of $\delta\nu = -1.4$ cm^{-1} from 1606.3 cm^{-1} to 1604.9 cm^{-1}. This shift is relatively large compared to that $\delta\nu$ of -0.5 cm^{-1} found in copolymer case. Furthermore, this peak exhibits a ~15% decrease in intensity between the two temperatures, as shown in Fig. 2 *b* and Fig. 4, the biggest relative change in intensity among all

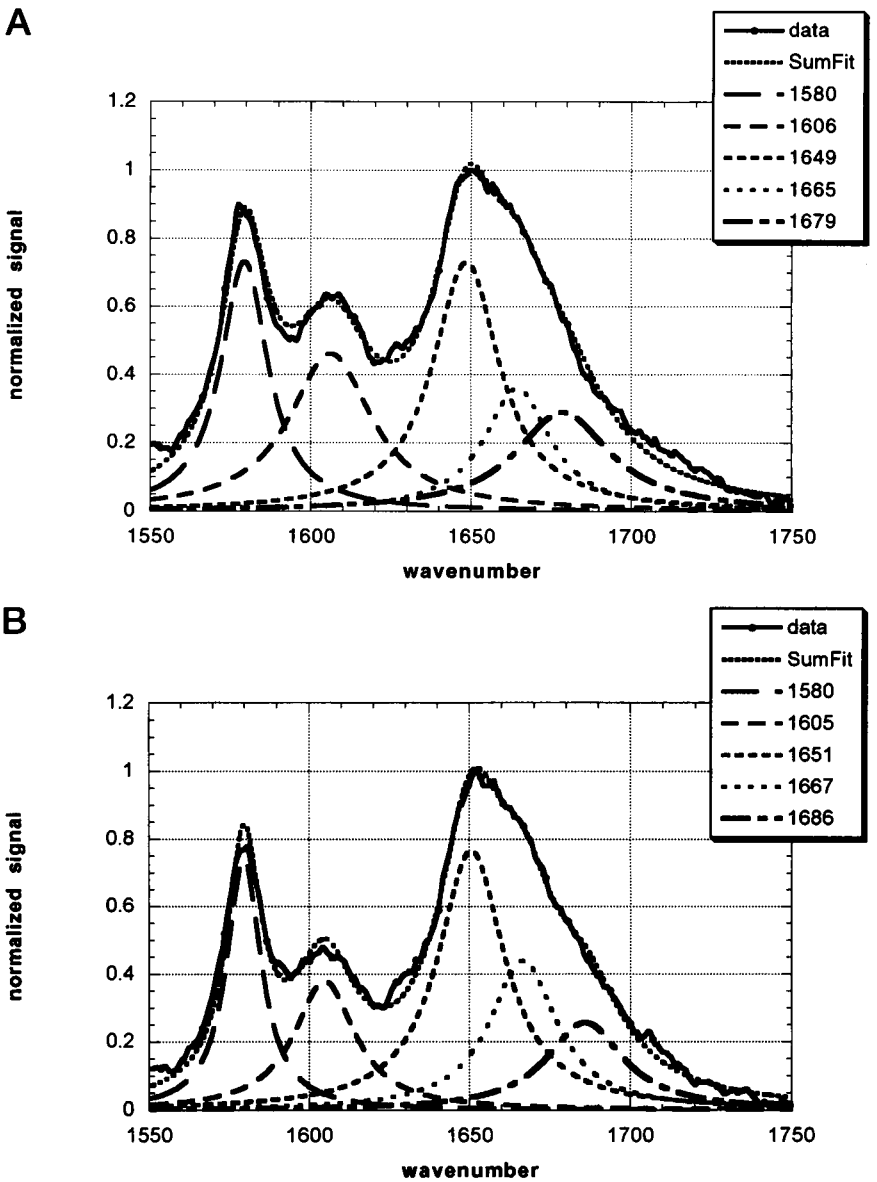

FIGURE 4 UVRR spectra from 1550 to 1750 cm^{-1} of poly(dA) · poly(dT) with Lorentzian fits using five peaks (*a*) at 5°C and (*b*) at 55°C. Solid lines are the data. All dashed and dotted-dashed lines are the curve fits, and the dotted lines are fits to the data, made by summing the five peaks. The reduced χ^2 is 2.7 for *a* and 2.1 for *b*.

peaks. The most significant effect can be seen in the $(C4{=}O)_B$ frequency of the thymine, which shows a large upshift, $\delta\nu = +7.2$ cm^{-1} between 5°C and 55°C. The $(C4{=}O)_A$ frequency also shifts up, but by a smaller amount, $+2.1$ cm^{-1}. Thus the dipole-dipole coupling changes with temperature, and the overall upshift implies an increase in the C4=O bond strength at 55°C. This change is in the direction expected for loss of a low-temperature H bond, as is the downshift in the NH_2 scissors mode. (The thymine C5=C6 stretch also shifts up 2.2 cm^{-1}, probably because of a C4=O contribution to this mode.)

Although it is not possible to at present show from calculations the expected frequency shifts due to three-center hydrogen bond formation, the UVRR results are clearly consistent with all of the previous findings that the low-temperature structure of poly(dA) · poly(dT) duplex is different from the high-temperature structure, and thus the premelting transition is observed, whereas poly[d(AT)] duplex has the same structure below the duplex melting temperature. From the curve fit spectral frequencies from 1550–1750 cm^{-1}, the high temperature state of homopolymer resembles the alternating copolymer at both high- and low-temperature limits. Furthermore, the concomitant shiftings of thymine C4=O stretch and adenine $N6H_2$ scissors mode plus its relative intensity decrease seem to support the idea that the changes can be explained by a third hydrogen bond formed cross-strand between consecutive dA · dT pairs at low temperature. This H bond could stabilize the extra amount of propeller twist between the A-T base planes. At physiological temperatures above 35°C, this bond breaks and the poly(dA) · poly(dT) becomes B-like DNA duplex.

DISCUSSION

The UVRR data provide strong evidence for the presence of a 3-centered hydrogen bond as the cause for anomalous

TABLE 1 Poly[d(AT)] Lorentzian fits of high-frequency bands

Peak no.	Assignment	Parameters	5°C	55°C	$\delta\nu$
1	A: C4═C5	ν (cm^{-1})	1578.1	1577.9	−0.2
		FWHM (cm^{-1})	13	13	—
		Area (%)	14	13	—
2	A: $N6H_2$	ν (cm^{-1})	1605.1	1604.6	−0.5
		FWHM (cm^{-1})	23	22	—
		Area (%)	27	25	—
3	T: $(C4{=}O)_A$	ν (cm^{-1})	1649.5	1649.8	+0.3
		FWHM (cm^{-1})	25	25	—
		Area (%)	32	37	—
4	T: C5═C6	ν (cm^{-1})	1665.5	1666.6	+1.1
		FWHM (cm^{-1})	25	25	—
		Area (%)	16	16	—
5	T: $(C4{=}O)_B$	ν (cm^{-1})	1684.5	1684.0	−0.5
		FWHM (cm^{-1})	32	26	—
		Area (%)	11	9	—

structure of poly(dA) · poly(dT) at and below ambient temperature; however, other causes have been advanced.

Changes in the ordered bound water molecules ("spine of hydration"), which have been found to be primarily localized in the minor groove region of duplexes, have been advanced by Prohofsky et al. as the origin of the unusual low-temperature structure of poly(dA) · poly(dT) (Chen and Prohofsky, 1993). We do not think that "bound water" can explain the main CD and DSC experimental results. Although "bound water" was initially thought to be A-tract specific, later evidence has shown that all bases can have bound water molecules in the minor groove (Berman, 1991; Schneider et al., 1992). Thus, unlike A-tract-specific 3-centered hydrogen bonds, the nonspecificity of "bound water" implies that somehow differences in how ordered the water molecules are and how far they are situated from the perimeter of the base atoms can explain base-pair-specific effects. Second, and more important, there is no clear two-state model for the bound water that can explain either the isosbestic (more precisely, isoelliptic) spectroscopic signatures of the transition or the sharpness of the transition that is associated with the duplex helical substructures.

TABLE 2 Poly(dA) · poly(dT) Lorentzian fits of high-frequency bands

Peak no.	Assignment	Parameters	5°C	55°C	$\delta\nu$
1	A: C4═C5	ν (cm^{-1})	1579.5	1579.9	+0.4
		FWHM (cm^{-1})	12	13	—
		Area (%)	20	17	—
2	A: $N6H_2$	ν (cm^{-1})	1606.3	1604.9	−1.4
		FWHM (cm^{-1})	23	23	—
		Area (%)	22	16	—
3	T: $(C4{=}O)_A$	ν (cm^{-1})	1648.6	1650.7	+2.1
		FWHM (cm^{-1})	25	25	—
		Area (%)	29	34	—
4	T: C5═C6	ν (cm^{-1})	1664.5	1666.7	+2.2
		FWHM (cm^{-1})	25	25	—
		Area (%)	14	20	—
5	T: $(C4{=}O)_B$	ν (cm^{-1})	1678.7	1685.9	+7.2
		FWHM (cm^{-1})	36	29	—
		Area (%)	15	13	—

Diekmann et al. (1992) have proposed that base-pair stacking interactions optimized by propeller twisting are responsible for the low-temperature structure seen in poly(dA) · poly(dT). This model comes from the observation that phased tracts with the sequence dAIAIA · dTCTCT also show retarded mobility, where I is the inosine nucleotide. This is a very puzzling result, because the alternating copolymer dATATA · dTATAT does *not* show retardation, and like the dAIAIA · dTCTCT sequence cannot form 3-centered hydrogen bonds. However, as Diekmann et al. point out, the dAIAIA · dTCTCT sequence is a form of a polypurine-polypyrimidine duplex, like poly(dA) · poly(dT), and should have similar base-pair stacking interactions. We are left with a puzzle: our UVRR results discussed here clearly show that in the case of poly(dA) · poly(dT) there is clear evidence for a 3-centered hydrogen bond at low temperatures, whereas none is seen in the alternating copolymer, in agreement with both our previous spectroscopic work and the gel retardation assays. At this point, we can only say that very little is known about the true structure of dAIAIA · dTCTCT in solution and its temperature-dependent structures. In this paper we have chosen to concentrate on the better understood and biologically occurring sequences.

Most recently and independently, Takeuchi and Sasamori (1995) have addressed similar issues of hydrogen bonding and base stacking of the polymer duplexes interacting with a tetrapeptide Ser-Pro-Lys-Lys, which are found repeatedly in histone H1 proteins using UVRR, including the comparison between 55°C and 22°C. Although their spectra were very similar to our measurements for the duplexes alone, we do not agree with the way difference spectra were obtained and the subsequent interpretations. However, we do agree with the authors that the structural changes seen in A-tracts can be caused by influences other than temperature, and thus this structural change can occur under isothermal in vivo conditions.

We have also tried to examine the UVRR spectra of the 45-bp duplex, which has four tracts of $(dA)_5$, using the same sample as the one used in the DSC and CD experiments (Chan et al, 1993). Unfortunately, the spectral bands have additional vibrational contributions from the guanine and cytosine bases. Although there are some spectral changes between low and high temperatures, it is impossible to deconvolute all of the bands to provide a clear and unambiguous analysis. Thus this part of the data is not presented in this paper.

CONCLUSIONS

We have observed only in poly(dA) · poly(dT) concomitant changes of both the thymine C4═O stretch and the adenine amino scissors mode as temperature increases. These changes are not to be confused with the triple helical tran-

sition that can happen if poly(dA) · poly(dT) is in high salt conditions. For the premelting transition, the UVRR evidence supports a breaking of a hydrogen in the major groove that is not a Watson-Crick bond but a third H bond, which is unique to a sequence with A-tracts. Therefore we can conclude that this premelting transition is due to the breaking of the bifurcated H bond cross-strand from adenine to the consecutive flanking thymine. This third H bond, in turn, can stabilize the extra propeller twist of the A-T base planes at temperatures below ambient. However, this bond becomes unstable above 35°C; thus the DNA segment will change its rigidity and become B-like, possibly becoming able to do biological transformation like condensing with histones to form nucleosomes. UV resonance Raman has given us, more specifically, the origin of the premelting transition that is unique to the A-T homopolymer or DNA with $(dA)_n$ tracts, as compared to the copolymer or randomized sequences.

RHA and SSC acknowledge support from National Science Foundation grant MCB-9202170, Office of Naval Research grant N00014-91-J-4084, and National Institutes of Health grant 1 R03 RR08032-01. TGS acknowledges support from National Institutes of Health grant GM 25158. The X-ray plots were obtained through the Nucleic Acid Database Project, Rutgers University, funded by NSF, with generous help from Dr. A. R. Srinivasan and Dr. Les Clowney.

REFERENCES

Arnott, S., R. Chandrasekaran, D. W. L. Hukins, P. J. C. Smith, and L. Watts. 1974. Structural details of a double-helix observed for DNAs containing alternating purine and pyrimidine sequences. *J. Mol. Biol.* 88:523–533.

Arnott, S., and E. Selsing. 1974. Structures for the polynucleotide complexes poly(dA) · poly(dT) and poly(dT) · poly(dA) · poly(dT). *J. Mol. Biol.* 88:509–521.

Aymami, J., M. Coll, C. A. Frederick, A. H.-J. Wang, and A. Rich. 1989. The propeller DNA conformation of poly(dA) · poly(dT). *Nucleic Acids Res.* 17:3229–3245.

Berman, H. M. 1991. Hydration of DNA. *Curr. Opin. Struct. Biol.* 1:423–427.

Chan, S. S., K. J. Breslauer, R. H. Austin, and M. E. Hogan. 1993. Thermodynamics and premelting conformational changes of phased $(dA)_5$ tracts. *Biochemistry.* 32:11776–11784.

Chan, S. S., K. J. Breslauer, M. E. Hogan, D. J. Kessler, R. H. Austin, J. Ojemann, J. M. Passner, and N. C. Wiles. 1990. Physical studies of DNA premelting equilibria in duplexes with and without homo dA · dT tracts: correlations with DNA binding. *Biochemistry.* 29:6161–6171.

Chen, Y. Z., and E. W. Prohofsky. 1993. Synergistic effects in the melting of DNA hydration shell: melting of the minor groove hydration spine in poly(dA) · poly(dT) and its effect on base pair stability. *Biophys. J.* 64:1385–1393.

Coll, M., C. A. Frederick, A. H.-J. Wang, and A. Rich. 1987. A bifurcated hydrogen-bonded conformation in the d(A · T) base pairs of the DNA dodecamer d(CGCAAATTTGCG) and its complex with distamycin. *Proc. Natl. Acad. Sci. USA.* 84:8385–8389.

Crothers, D. M., and J. Drak. 1992. Global features of DNA. structure by comparative gel electrophoresis. *Methods Enzymol.* 212:46–71.

Diekmann, S., J. M. Mazzarelli, L. W. McLaughlin, E. von Kitzing, and A. V. Travers. 1992. DNA curvature does not require bifurcated hydrogen bonds or pyrimidine groups. *J. Mol. Biol.* 225:729–738.

Diekmann, S., and J. C. Wang. 1985. On the sequence determinants and flexibility of the kinetoplast DNA fragment with abnormal gel electrophoretic mobilities. *J. Mol. Biol.* 86:1–11.

Fodor, S. P. A., R. P. Rava, T. R. Hays, and T. G. Spiro. 1985. Ultraviolet resonance Raman spectroscopy of the nucleotides with 266-, 240-, 218-, and 200-nm pulsed laser excitation. *J. Am. Chem. Soc.* 107:1520–1529.

Fodor, S. P. A., and T. G. Spiro. 1986. Ultraviolet resonance Raman spectroscopy of the DNA with 200–266-nm laser excitation. *J. Am. Chem. Soc.* 108:3198–3205.

Grygon, C. A., and T. G. Spiro. 1990. UV resonance Raman spectroscopy of nucleic acid duplexes containing A-U and A-T base pairs. *Biopolymers.* 29:707–715.

Hagerman, P. J. 1986. Sequence-directed curvature of DNA. *Nature.* 321:449–450.

Herrera, J. E., and J. B. Chaires. 1989. A premelting conformational transition in poly(dA)-poly(dT) coupled to daunomycin binding. *Biochemistry.* 26:1993–2000.

Nelson, H. C. M., J. T. Finch, B. F. Luisi, and A. Klug. 1987. The structure of an oligo(dA)-oligo(dT) tract and its biological implications. *Nature.* 330:221–226.

Perno, J. R., C. A. Grygon, and T. G. Spiro. 1989. Ultraviolet Raman excitation profiles for the nucleotides and the nucleic acid duplexes poly(rA)-poly(rU) and poly(dG-dC). *J. Phys. Chem.* 93:5672–5678.

Peticolas, W. L., and E. Evertsz. 1992. Conformation of DNA in vitro and in vivo from laser Raman scattering. *Methods Enzymol.* 211:335–352.

Schneider, B., D. Cohen, and H. M. Berman. 1992. Hydration of DNA bases: analysis of crystallographic data. *Biopolymers.* 32:725–750.

Stellwagen, A., and N. C. Stellwagen. 1990. Anomalously slow electrophoretic mobilities of DNA restriction fragments in polyacrylamide gels are not eliminated by increasing the gel pore size. *Biopolymers.* 30: 309–324.

Takeuchi, H., and J. Sasamori. 1995. Structural modification of DNA by a DNA-binding motif SPKK: detection of changes in base-pair hydrogen bonding and base stacking by UV resonance Raman spectroscopy. *Biopolymers.* 35:359–367.

Thomas, G. J., Jr., and J. Livramento. 1975. Kinetics of hydrogen-deuterium exchange in adenosine 5′-monophosphate, adenosine 3′:5′-monophosphate, and poly(riboadenylic acid) determined by laser-Raman spectroscopy. *Biochemistry.* 23:5210–5218.

Toyama, A., H. Takeuchi, and I. Harada. 1991. Ultraviolet resonance Raman spectra of adenine, uracil and thymine derivatives in several solvents. Correlation between band frequencies and hydrogen-bonding states of the nucleic acid bases. *J. Mol. Struct.* 242:87–98.

Tsuboi, M. 1985. Detailed structure of DNA duplexes in solution as revealed by its vibrational spectrum. *In* Spectroscopy of Biological Molecules. J. P. Alia, L. Bernard, and Manfiat, editors. Wiley, Chichester. 101–107.

Tsuboi, M., and Y. Nishimura. 1982. Recent development in the Raman spectroscopy of nucleic acids. *In* Raman Spectroscopy, Linear and Nonlinear. J. Lascombe and P. V. Huong, editors. Wiley, Chichester. 683–693.

Tsuboi, M., Y. Nishimura, A. Y. Hirakawa, and W. L. Peticolas. 1987. Resonance Raman spectroscopy and normal modes of the nucleic acid bases. *In* Biological Applications of Raman Spectroscopy, Vol. 2. T. G. Spiro, editor. John Wiley, New York. 109–179.

Tsuboi, M., and S. Takahashi. 1973. Infrared and Raman spectra of nuclei acids—vibrations in the base-residues. *In* Physico-Chemical Properties of Nucleic Acids, Vol. 2. J. Duchesne, editor. Academic Press, New York. 91–145.

Yoon, C., G. G. Prive, D. S. Goodsell, and R. E. Dickerson. 1988. Structure of an alternating-B DNA helix and its relationship to A-tract DNA. *Proc. Natl. Acad. Sci. USA.* 85:6332–6336.